MA Hongwei, XU Lie, LI Yongdong

Tsinghua University

Research on the Direct Power Control Based Multi-objective Control for DFIG Asymmetrical LVRT

Abstract. *This paper proposes a novel control strategy for doubly fed induction generator (DFIG) low voltage ride through (LVRT) under asymmetrical grid voltage dip. The proposed strategy, named as direct power control based multi-objective control, enables the DFIG operating under asymmetrical grid voltage dip and operating at different control objectives (the current distortion limitation mode, the power oscillation limitation mode and the torque oscillation limitation mode) by adjusting only one parameter. Furthermore, the proposed method can achieve a smooth switch between the steady state operation and the voltage dip operation with an improved dynamic performance. The simulation results verify the correction and effectiveness of the proposed method.*

Streszczenie. *W artykule przedstawiono nową metodę sterowania generatorem DFIG, pracującym przy przejściowo niskim napięciu. Proponowany algorytm umożliwia pracę w takich warunkach, poprzez zmianę nastawy tylko jednego parametru. Osiągnięto płynność przejścia między stanem ustalonym a stanem zapadu napięcia. Przedstawiono wyniki badań symulacyjnych, potwierdzające skuteczność rozwiązania. (**Sterowanie wielokryteriowe maszyną DFIG przy asymetrycznych zapadach napięcia LVRT, bazujące na bezpośrednim sterowaniu mocą**).*

Keywords: Doubly fed induction generator (DFIG), direct power control (DPC), multi-objective control, low voltage ride through (LVRT), asymmetrical voltage dip.
Słowa kluczowe: DFIG, bezpośrednie sterowanie mocą, sterowanie wielokryteriowe, praca przy niskim napięciu, LVRT, asymetryczny zapad napięcia.

Introduction

Due to the merits in the reduced converter capacity, cost and volume, the variable speed operation, reduced power losses compared to other solutions such as fixed speed induction generators or synchronous generators, the DFIG acts as an important role in wind power system [1, 2]. A typical DFIG-based wind power system is shown in Fig.1. The DFIG control algorithms and the relative LVRT strategies gain an increasing attention in recent decades. Varieties of control algorithms have been proposed in literatures and the classic control algorithms are either field-oriented vector control [3-6] or direct control [1, 7-13]. The field-oriented vector control generally consists of the stator-voltage-oriented vector control [3, 4] and the stator-flux-oriented vector control [5, 6]. The direct control consists of direct torque control (DTC) [7-9] or the direct power control (DPC) [1, 10-13]. In literatures, the direct torque control [8, 9] and the direct power control [10, 11] are verified to be a suitable method for DFIG system. The direct controls are demonstrated to obtain a significantly improved dynamic performance and high robust for DFIG system. Also, the direct controls do not need current regulators, the complex rotational coordinate transformations and the specific modulations. Furthermore, the direct control algorithms also reduce the complexity in practical application and minimize the requirement of DFIG parameters. In a DFIG system, the stator is directly connected to the power grid, which results the system sensitive to the grid voltage disturbances. An abrupt grid voltage drop can lead to the over voltage and over current at both DFIG rotor windings and the converter. Initially, the solution of the low voltage ride through is to short-circuit the rotor windings with the crowbar and disconnect the DFIG to the grid [2]. Unfortunately, this method may aggravate the grid voltage dip. Therefore, it is important to enable the LVRT capability for the DFIG-based wind power systems when grid voltage dips. Considering the LVRT acts as an important role in practical DFIG system and the asymmetrical voltage dip occurs more regularly than symmetrical voltage dip in practical applications, this paper focus on the direct power control based multi-objective control for DFIG asymmetrical LVRT. Some authors decompose the DFIG model with both positive and negative sequence
models and apply the classic vector control for both models separately. It benefits in understanding the control structures but double the PI controllers for current loops.

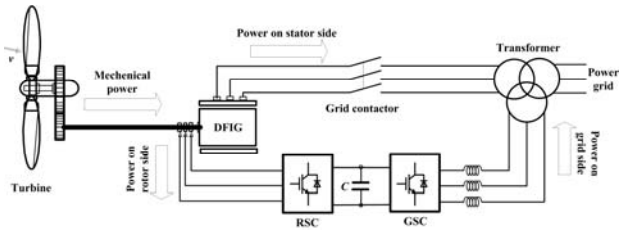

Fig.1. Typical DFIG-based wind power system

Also, the control algorithm based on disturbance rejection controllers is proposed to compensate the oscillations produced by the asymmetrical voltage dip, by inserting a feed forward component to the current controllers. Furthermore, an alternative DPC strategy for DFIG under asymmetrical voltage conditions are also proposed with optimal control theory. Different control objectives are considered during LVRT, but the calculation quantities are large, which makes it complex in practical application. In normal operation, the objective of the DPC algorithm for a DFIG system is to control the system output power and a unit power factor. However, in asymmetrical grid voltage dip conditions, the above control target becomes less obvious because the stator current is no longer sinusoidal in asymmetrical voltage dip condition [11]. Considering the requirement of the DFIG, the different control objectives during LVRT can be:

- The constant stator active and reactive power;
- The constant electrical torque;
- The sinusoidal stator current and the constant reactive power;
- A combination of the above three control objectives.

The proposed direct power control based multi-objective control has the following characteristics:

- direct stator active and reactive power control without inner current loops;
- only two multi-frequency proportional integral resonant controllers (MFPIRs) are employed;
- multiply objectives are achieved by adjusting only one parameter λ between 0 and 2;

This paper is organized in following sections. In Section II, the characteristics of DFIG under asymmetrical voltage dip is discussed. In Section III, the direct power control based multi-objective control for DFIG under asymmetrical voltage dip is presented in detail. Simulation results are provided to verify the proposed strategy in Section IV. Conclusion is given in Section V.

Behavior of DFIG under asymmetrical voltage dip

According to the symmetrical components theory, any three-phase sinusoidal system can be decomposed as three separated and balanced sub-systems, which are the positive, negative and zero sequences. It means any electromagnetic quantity can be expressed in the form of:

(1) $$\overrightarrow{F} = \overrightarrow{F_0} + \overrightarrow{F_+} + \overrightarrow{F_-}$$

where: F -the target electromagnetic quantity, the subscripts "0", "+" and "–" represent the zero, positive and negative components respectively.

The positive and negative dq reference frames in the vector space can be constructed as Fig.2. The positive sequence dq$^+$ frame rotates at the synchronous speed ω_e while the negative sequence dq$^-$ frame rotates at the speed of $-\omega_e$. Then the transformations between $\alpha\beta$, dq^0, dq$^+$ and dq$^-$ frame are given as

(2) $$\overrightarrow{F}^0 = \overrightarrow{F}^{\alpha\beta}, \overrightarrow{F}^+ = \overrightarrow{F}^{\alpha\beta} e^{-j\omega_e t}, \overrightarrow{F}^- = \overrightarrow{F}^{\alpha\beta} e^{j\omega_e t}$$

(3) $$\overrightarrow{F}^+ = \overrightarrow{F}^- e^{-j2\omega_e t}, \overrightarrow{F}^- = \overrightarrow{F}^+ e^{j2\omega_e t}$$

where the superscripts "0", "+" and "–" indicate the vector in dq^0, dq$^+$ and dq$^-$ frame respectively. Therefore, (1) can be written as (4) in dq+ frame.

(4) $$\overrightarrow{F}^+ = \overrightarrow{F_+}^+ + \overrightarrow{F_0}^+ e^{-j\omega_e t} + \overrightarrow{F_-}^- e^{-j2\omega_e t}$$

From (4), it can be found that an asymmetrical electromagnetic quantity consists of dc, synchronous frequency and double synchronous frequency components in the view of dq$^+$ frame.

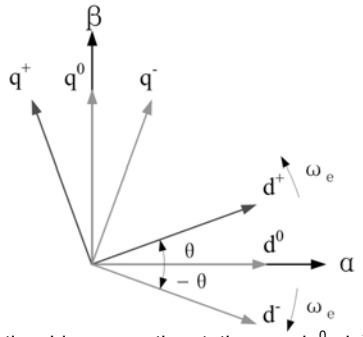

Fig.2. The relationship among the stationary, dq^0, dq$^+$ and dq$^-$ frame

Using grid voltage as an example (Fig 3), the symmetrical grid voltage is shown as the big circle in vector space. When grid voltage becomes asymmetrical, it is described as the ellipse and it can be composed as positive sequence and the negative sequence as shown in Fig.3.

In this case, it is obvious that the control algorithm for asymmetrical voltage dip is to restrain the effect of the negative sequence component, which results in the system oscillation at twice synchronous frequency.

The equivalent DFIG circuit in dq$^+$ reference frame rotating at synchronous speed is shown in Fig.4.

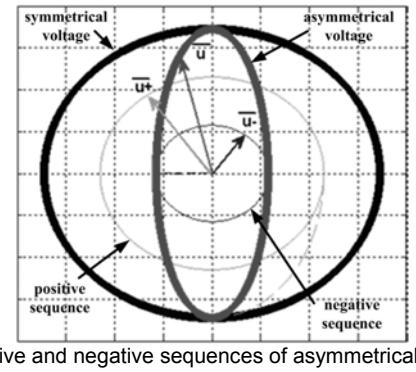

Fig. 3 Positive and negative sequences of asymmetrical voltage

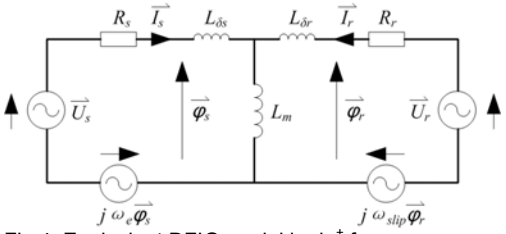

Fig.4. Equivalent DFIG model in dq$^+$ frame

Under normal grid conditions, the DFIG can be expressed as Park's model.

(5) $$\overrightarrow{U_s} = R_s \overrightarrow{I_s} + \frac{d\overrightarrow{\varphi_s}}{dt} + j\omega_e \overrightarrow{\varphi_s}$$

(6) $$\overrightarrow{U_r} = R_s \overrightarrow{I_r} + \frac{d\overrightarrow{\varphi_r}}{dt} + j\omega_{slip} \overrightarrow{\varphi_r}$$

(7) $$\overrightarrow{\varphi_s} = L_s \overrightarrow{I_s} + L_m \overrightarrow{I_r}$$

(8) $$\overrightarrow{\varphi_r} = L_r \overrightarrow{I_r} + L_m \overrightarrow{I_s}$$

(9) $$P_s + jQ_s = \overrightarrow{U_s}\,\overrightarrow{I_s}^*$$

(10) $$T_e = n_p \overrightarrow{\varphi_s} \times \overrightarrow{I_s}$$

When asymmetrical voltage dip occurs, the behavior of DFIG can be studied by the method of symmetrical components theory introduced previously. According to the theory, the asymmetrical voltage on stator can be expressed as a sum of three components: positive, negative and zero sequences. Zero sequence voltage usually does not affect the machine since they are typically connected to delta-star transformers, therefore only the positive and negative sequence components are necessary. In this case, the stator voltage can be written as

(11) $$\overrightarrow{U_s}^+ = \overrightarrow{U_{s+}}^+ + \overrightarrow{U_{s-}}^+ = \overrightarrow{U_{s+}}^+ + \overrightarrow{U_{s-}}^- e^{-j2\omega_e t}$$

Under symmetrical grid voltage, the stator flux vector rotates at the synchronous speed, which means the stator flux only consists of positive component only. However, if the asymmetrical voltage dip occurs, negative and zero sequence components will be injected into the stator flux. Assuming the voltage dip at time of t_0, from (5)-(8) and (11), it can be obtained that the transient stator flux vector can be rewritten as

(12) $$\overrightarrow{\varphi_s}^+ = \overrightarrow{\varphi_{s0}}^+ + \overrightarrow{\varphi_{s+}}^+ + \overrightarrow{\varphi_{s-}}^+$$

where:

$$\overrightarrow{\varphi}_{s0}^{+}=\frac{\overrightarrow{U}_{s}^{+}(t_0-)-\overrightarrow{U}_{s+}^{+}(t_0+)+\overrightarrow{U}_{s-}^{+}(t_0+)}{j\omega_e}e^{-t/T_s'}e^{-j\omega_e t}$$

$$\overrightarrow{\varphi}_{s+}^{+}=\frac{\overrightarrow{U}_{s+}^{+}(t_0+)}{j\omega_e}$$

$$\overrightarrow{\varphi}_{s-}^{+}=\frac{\overrightarrow{U}_{s-}^{+}(t_0+)}{-j\omega_e}e^{-j2\omega_e t}$$

In (12), $\overrightarrow{\varphi}_{s0}^{+}$, $\overrightarrow{\varphi}_{s+}^{+}$ and $\overrightarrow{\varphi}_{s-}^{+}$ indicate the zero, positive and negative sequence components of stator flux vector, respectively. The symbol t_{0-} and t_{0+} indicate the transition before and after voltage dip respectively. $\overrightarrow{U}_{s}^{+}(t_0-)$, $\overrightarrow{U}_{s+}^{+}(t_0+)$ and $\overrightarrow{U}_{s-}^{+}(t_0+)$ are the original stator voltage before voltage dip, the positive and negative sequence components of stator voltage vector after voltage dip respectively. Among the sequential components of stator flux vector, $\overrightarrow{\varphi}_{s0}^{+}$ is determined by the constant flux linkage theory and it will be damped with the stator transient time constant T_s'. The dynamic behavior of the stator flux under asymmetrical voltage dip can be present in Fig.5.

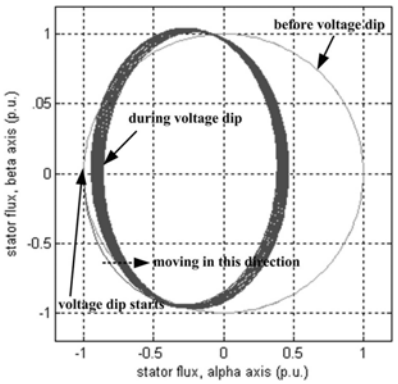

Fig.5. Stator flux trajectory for an 50% single-phase voltage dip

The sequential components of DFIG stator flux will induce the relative sequential flux components at the rotor side. From (7) and (8), the sequential of rotor and stator flux can lead to the unexpected components at stator and rotor current, the electromagnetic torque and power. This process can be presented in Fig.6 and derived in mathematics as follows. From (4), (11) and Fig.2, the stator current of DFIG under asymmetrical voltage dip can be expressed as follows:

(13) $$\overrightarrow{I}_{s}^{+}=\overrightarrow{I}_{s0}^{+}+\overrightarrow{I}_{s+}^{+}+\overrightarrow{I}_{s-}^{+}=\overrightarrow{I}_{s+}^{+}+\overrightarrow{I}_{s0}^{0}e^{-j\omega_e t}+\overrightarrow{I}_{s-}^{-}e^{-j2\omega_e t}$$

where $\overrightarrow{I}_{s0}^{dq+}$ is caused by $\overrightarrow{\varphi}_{s0}^{dq+}$ shown in (11) and $\overrightarrow{I}_{s0}^{dq+}$ is also damped with the stator transient time constant T_s'.

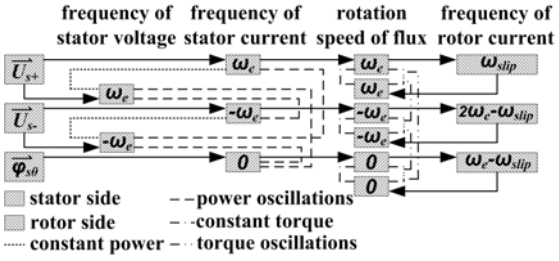

Fig.6. Various components of electromagnetic quantities and their interaction in DFIG under transient asymmetrical voltage dip

Substituting (11) and (13) into (9), it can be obtained that:

(14) $$P_s+jQ_s=\overrightarrow{U}_s\overrightarrow{I}_s^{*}=\left(\overrightarrow{U}_{s+}^{+}+\overrightarrow{U}_{s-}^{-}e^{-j2\omega_e t}\right)\left(\overrightarrow{I}_{s+}^{+}+\overrightarrow{I}_{s0}^{0}e^{-j\omega_e t}+\overrightarrow{I}_{s-}^{-}e^{-j2\omega_e t}\right)^{*}$$

Then the stator power can be expressed as:

(15) $$P_s=P_{scons}+P_{s\omega_e}+P_{s2\omega_e}$$

(16) $$Q_s=Q_{scons}+Q_{s\omega_e}+Q_{s2\omega_e}$$

where:

$$P_{scons}+jQ_{scons}=\overrightarrow{U}_{s+}^{+}\overrightarrow{I}_{s+}^{+*}+\overrightarrow{U}_{s-}^{-}\overrightarrow{I}_{s-}^{-*}$$

$$P_{s\omega_e}+jQ_{s\omega_e}=\overrightarrow{U}_{s+}^{+}\overrightarrow{I}_{s0}^{0*}e^{j\omega_e t}+\overrightarrow{U}_{s-}^{-}\overrightarrow{I}_{s0}^{0*}e^{-j\omega_e t}$$

$$P_{s2\omega_e}+jQ_{s2\omega_e}=\overrightarrow{U}_{s+}^{+}\overrightarrow{I}_{s-}^{-*}e^{j2\omega_e t}+\overrightarrow{U}_{s-}^{-}\overrightarrow{I}_{s+}^{+*}e^{-j2\omega_e t}$$

Based on (15) and (16), it can be found that under the asymmetrical voltage dip, the stator power includes not only the constant average components (P_{scons} and Q_{scons}), but also the fundamental grid frequency oscillations ($P_{s\omega_e}$ and $Q_{s\omega_e}$) and double grid frequency oscillations ($P_{s2\omega_e}$ and $Q_{s2\omega_e}$). Substituting (12) and (13) into (10), the electromagnetic torque is given as

(17) $$\begin{aligned}T_e&=n_p\overrightarrow{\varphi}_s\times\overrightarrow{I}_s\\&=n_p\left(\overrightarrow{\varphi}_{s0}^{0}e^{-j\omega_e t}+\overrightarrow{\varphi}_{s+}^{+}+\overrightarrow{\varphi}_{s-}^{-}e^{-j2\omega_e t}\right)\times\left(\overrightarrow{I}_{s+}^{+}+\overrightarrow{I}_{s0}^{0}e^{-j\omega_e t}+\overrightarrow{I}_{s-}^{-}e^{-j2\omega_e t}\right)\end{aligned}$$

Then the electromagnetic torque can be expressed as

(18) $$T_e=T_{econs}+T_{e\omega_e}+T_{e2\omega_e}$$

where

$$T_{econs}=n_p\left(\overrightarrow{\varphi}_{s+}^{+}\times\overrightarrow{I}_{s+}^{+}+\overrightarrow{\varphi}_{s-}^{-}\times\overrightarrow{I}_{s-}^{-}+\overrightarrow{\varphi}_{s0}^{0}\times\overrightarrow{I}_{s0}^{0}\right)$$

$$T_{e\omega_e}=n_p\left[e^{j\omega_e t}\times\left(\overrightarrow{\varphi}_{s0}^{0}\overrightarrow{I}_{s+}^{+}+\overrightarrow{\varphi}_{s-}^{-}\overrightarrow{I}_{s0}^{0}\right)+e^{-j\omega_e t}\times\left(\overrightarrow{\varphi}_{s0}^{0}\overrightarrow{I}_{s-}^{-}+\overrightarrow{\varphi}_{s+}^{+}\overrightarrow{I}_{s0}^{0}\right)\right]$$

$$T_{e2\omega_e}=n_p\left(e^{-j2\omega_e t}\times\overrightarrow{\varphi}_{s+}^{+}\overrightarrow{I}_{s-}^{-}+e^{j2\omega_e t}\times\overrightarrow{\varphi}_{s-}^{-}\overrightarrow{I}_{s+}^{+}\right)$$

From (18), it can be known that the fundamental and double grid frequency oscillations also exist in electromagnetic torque.

III. DPC Based multi-objective control

From previous analysis, the DPC based multi-objective control can be illustrated as Fig.7.

- When λ=0, Ps和Qs are controlled as given constant values, hence the power oscillation are control to zero;
- When λ=1, Ps+ and Qs+ are controlled to the desired values, hence leads to best sinusoidal shaped stator current;
- When λ=2, the Pte and Qs are controlled to the desired values, hence the torque and reactive power ripple demonstrates the best performance;

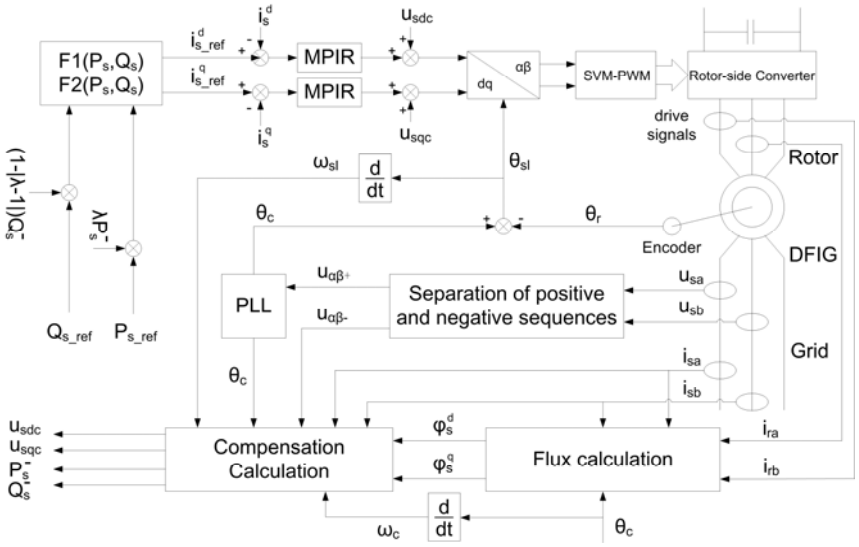

Fig.7. control diagram of DPC based multi-objective control

IV. Simulation results

To validate the theoretical findings, the following simulation are presented:

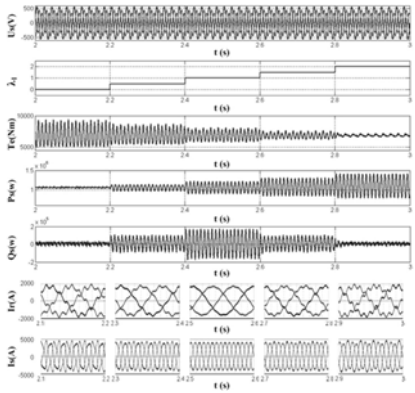

Fig.8 Dynamic behaviour of multi-objective control (Asymmetrical Factor = 15%)

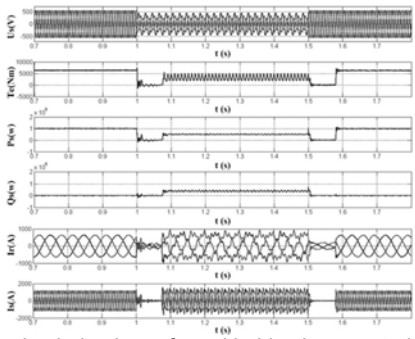

Fig.9 Dynamic behavior of multi-objective control for LVRT (Asymmetrical Factor = 20%)

In fig 8 and 9, the different λ values are given and the relative results, which include stator currents, torque, active and reactive powers, are presented to validate the multi-objective control algorithm.

Conclusion

The dynamic behaviour of the LVRT is firstly discussed in this paper. The DPC based multi-objective control is presented in this paper to achieve different control target during LVRT for DFIG system. The simulation results are given to demonstrate the validity of the DFIG system and verify the proposed control algorithm.

REFERENCES

[1] J. Hu, H. Nian, B. Hu, Y. He and Z. O. Zhu, Direct active and reactive power regulation of DFIG using sliding-mode control approach, IEEE Transactions on Energy Conversion, 25 (2010), No. 4, 1028-1039

[2] M. Tazil, V. Kumar, R. C. Bansal, S. Kong, Z. Y. Dong, W. Freitas, H. D. Mathur, Three-phase doubly fed induction generators: an overview, IET Electric Power Application, 4 (2010), No. 2, 75-89

[3] H. Akagi and H. Sato, Control and performance of a doubly-fed induction machine intender for a flywheel energy storage system, IEEE Transactions on Power Electronics, 17 (2002), No. 1, 109-116

[4] T. K. A. Brekken, N. Mohan, Control of a doubly fed induction wind generator under unbalanced grid voltage conditions, IEEE Transacions on Energy Conversion, 22 (2007), No. 1, 129-135

[5] M. Mohseni, S. M. Islam and M. A. Masoum, Enhanced hysteresis-based current regulators in vector control of DFIG wind turbines, IEEE Transactions on Power Electronics, 26 (2011), No. 1, 223-234

[6] G. D. Marques, D. M. Sousa, Air-gap-power-vector-based sensorless method for DFIG control without flux estimator, IEEE Transactions on Industrial Electronics, 58 (2011), No. 10, 4717-4726

[7] I. Takahashi and T. Noguchi, A new quick-response and high-efficiency control strategy of an induction motor, IEEE Transactions on Industrial Applications, IA-22 (1986), No. 5, 820-827

[8] G. S. Buja and M. P. Kazmierkowski, Direct torque control of PWM inverter-fed AC motors – A survey, IEEE Transactions on Industrial Electronics, 51 (2004), No. 4, 744-757

[9] Z. Liu, O. A. Mohammed and S. Liu, A novel direct torque control of doubly-fed induction generator used for variable speed wind power generation, Conf. Rec. IEEE Power Eng. Soc. Gen. Meeting (2007), 1-6

[10] L. Xu and P. Cartwright, Direct active and reactive power control of DFIG for wind energy generation, IEEE Transacions on Energy Conversion, 21 (2006), No. 3, 750-758

MA Hongwei: Phd student. Room 2-302, West main building, Tsinghua University, Beijing, China, 100086. E-mail: mhw08@mails.tsinghua.edu.cn.

XU Lie: Research assistant. Room 2-302, West main building, Tsinghua University, Beijing China, 100086. E-mail: xulie@mail.tsinghua.edu.cn.

LI Yongdong: Professor, Phd Supervisor. Room 2-304, West main building, Tsinghua University, Beijing, China, 100086. E-mail: liyd@mail.tsinghua.edu.cn.